Photocatalytic reduction of CO2 with H2O over graphene oxide-supported oxygen-rich TiO2 hybrid photocatalyst under visible light irradiation

Photocatalytic Reduction of CO_2 with H_2O Over Graphene Oxide–Supported Oxygen–Rich TiO_2 Hybrid Photocatalyst Under Visible Light Irradiation: Process and Kinetic Studies

Lling-Lling Tan, Wee-Jun Ong, Siang-Piao Chai, Abdul Rahman Mohamed

PII: S1385-8947(16)31286-4
DOI: http://dx.doi.org/10.1016/j.cej.2016.09.050
Reference: CEJ 15760

To appear in: *Chemical Engineering Journal*

Received Date: 23 June 2016
Revised Date: 1 September 2016
Accepted Date: 10 September 2016

Please cite this article as: L-L. Tan, W-J. Ong, S-P. Chai, A. Rahman Mohamed, Photocatalytic Reduction of CO_2 with H_2O Over Graphene Oxide–Supported Oxygen–Rich TiO_2 Hybrid Photocatalyst Under Visible Light Irradiation: Process and Kinetic Studies, *Chemical Engineering Journal* (2016), doi: http://dx.doi.org/10.1016/j.cej.2016.09.050

Photocatalytic Reduction of CO_2 with H_2O Over Graphene Oxide–Supported Oxygen–Rich TiO_2 Hybrid Photocatalyst Under Visible Light Irradiation: Process and Kinetic Studies

Lling-Lling Tan[a], Wee-Jun Ong[b], Siang-Piao Chai[c] and Abdul Rahman Mohamed[d]*

[a]Chemical Engineering, School of Engineering and Physical Sciences, Heriot-Watt University, Jalan Venna P5/2, Precinct 5, 62200 Putrajaya, Wilayah Persekutuan Putrajaya, Malaysia.

[b]Institute of Materials Research and Engineering (IMRE), Agency for Science, Technology and Research (A*STAR), 2 Fusionopolis Way, Innovis, 138634, Singapore.

[c]Multidisciplinary Platform of Advanced Engineering, Chemical Engineering Discipline, School of Engineering, Monash University, Jalan Lagoon Selatan, 46500 Bandar Sunway, Selangor, Malaysia.

[d]Low Carbon Economy (LCE) Group, School of Chemical Engineering, Universiti Sains Malaysia, Engineering Campus, Seri Ampangan, 143000 Nibong Tebal, Pulau Pinang, Malaysia.

*Corresponding author:
Tel: +603-55146234; Fax: +603-55146207
E-mail address: chai.siang.piao@monash.edu

Abstract

The photoreduction of carbon dioxide (CO_2) into hydrocarbon fuels was studied in a homemade photocatalytic system over 5 wt. % graphene oxide-doped oxygen-rich TiO_2 (5GO-OTiO_2) photocatalyst. The CO_2 transformation process is a sequential combination of both water oxidation and CO_2 reduction. As these processes can be affected by parameters such as radiant flux intensity and the partial pressures of both CO_2 and water vapour, these factors were systematically varied and studied in order to determine the most suitable process conditions for achieving high photocatalytic activity. Based on results from the CO_2 photoreduction experiments, a total methane (CH_4) yield of 3.450 μmol g_{cat}^{-1} was successfully attained over 5GO-OTiO_2 after 8 h of reaction time under visible light irradiation. The experimental data obtained was then fitted into the Langmuir-Hinshelwood surface reaction mechanism, wherein both CO_2 and H_2O adsorbed simultaneously on the photocatalyst surface to form the CH_4 product. Regression fitting was performed to determine the kinetic parameters such as reaction rate constant and adsorption equilibrium constants. The reaction rate as well as CO_2 and H_2O adsorption equilibrium constants were determined to be 84.42 μmol g_{cat}^{-1} h^{-1}, 0.019 bar^{-1} and 8.07 bar^{-1}, respectively. The significantly smaller CO_2 adsorption equilibrium constant implied that the adsorption of CO_2 was very weak while water strongly adsorbed on the photocatalyst surface.

Keywords: Graphene oxide, oxygen-rich, photocatalyst, carbon dioxide, process study, kinetics

1. Introduction

Fossil fuels are the major energy source used today and are rapidly consumed to meet the increasing energy demands of mankind. At the same time, carbon dioxide (CO_2), an inevitable product of fossil fuel combustion, leads to possible climate change and result in serious impacts to the environment [1-5]. Therefore, the ability to harness the power of CO_2 on a large scale and integrate it back into the utilization cycle as a sustainable form of energy production is highly desirable. Among the various renewable projects to date, the photocatalytic reduction of CO_2 into energy-bearing products has garnered interdisciplinary research attention to mitigate the ever-growing CO_2 concentration and to meet the long-term worldwide energy demands without utilizing further CO_2-generating power resources [6-15]. In this context, photocatalysis, a well-orchestrated mimic of natural photosynthesis, for direct conversion of solar energy to chemical energy, presents an opportunity to kill these two birds with one stone [16-19]. However, the state-of-the-art technology is far from being optimal due to low overall photoconversion and selectivity [20-22]. Hence, breakthroughs in the fabrication of highly efficient photocatalysts are necessary towards realizing the process for industrial applications.

Among the semiconductors that have been studied as photocatalysts for CO_2 reduction, titanium dioxide (TiO_2) is regarded as the most feasible in terms of its inexpensiveness, non-toxicity, high redox potentials and abundance [23-28]. Despite that, pure unmodified TiO_2 suffers from several drawbacks such as low quantum efficiency resulting from rapid recombination of charge carriers and the limit to UV-light absorption due to its wide band gap [29-33]. Great endeavours have been made to resolve these drawbacks, including cationic metal and anionic doping to manipulate the properties of TiO_2 [34-44]. However, these techniques could result in the generation of secondary impurities and oxygen vacancies, respectively, which could ultimately

reduce the photocatalytic activity of TiO_2 [45, 46]. Under such circumstances, it becomes a necessity to develop an effective synthetic route to fabricate visible-light-responsive and stable TiO_2 without the production of oxygen vacancies and secondary phases. In view of this, our research group has recently employed a dopant-free strategy to prepare a novel oxygen-rich TiO_2 (O_2-TiO_2) photocatalyst with significantly enhanced photocatalytic performance [47, 48]. By introducing oxygen excess defects into the lattice of TiO_2, the surface disorderliness caused an upshift of VB which led to a reduction of band gap energy from 3.2 eV to 2.95 eV. The resulting O_2-TiO_2 could then be activated by visible light, generating electron-hole pairs on its surface. Although O_2-TiO_2 showed remarkable efficiency in reducing CO_2 into methane (CH_4), its photocatalytic activity was observed to gradually deteriorate over time. This problem was successfully addressed by incorporating graphene oxide (GO) with O_2-TiO_2 *via* a wet chemical impregnation technique [10]. In the graphene oxide/oxygen-rich TiO_2 (GO-OTiO_2) hybridized material, GO served as a sink for electrons and an effective charge transporting bridge owing to its high electron mobility and extended -electron conjugation. The Schottky barrier formed at the interface of both components separated the photoinduced electron-hole pairs and decreased the charge recombination rate, which in turn improved the photostability of the hybrid composite significantly [10-12, 49, 50].

Our previous results showed that GO-OTiO_2 with an optimum GO loading of 5 wt. % exhibited the highest photoactivity towards CO_2 reduction. The total product yield obtained over GO-OTiO_2 was found to be 14.0 folds higher in comparison to commercial Degussa P25 [10]. Nevertheless, the fundamental mechanism of photocatalytic CO_2 reduction on GO-OTiO_2 photocatalyst has yet to be explored so far. In overall, the CO_2 conversion process is a sequential combination of both water oxidation and CO_2 reduction [8, 20, 51, 52]. These processes can be

affected substantially under different experimental conditions such as the intensity and wavelength of the incident light, reactor configuration, residence time as well as the partial pressures of the reactants, *i.e.* CO_2 and water vapour [53-60]. Therefore, in the present work, parameters including incident light intensity as well as the partial pressures of CO_2 and water vapour were systematically varied and studied in order to determine their effects on the CO_2 photoreduction process. In heterogeneous photocatalytic processes, rates are typically proportional to the adsorption of reactant molecules with efficient desorption of products from the surface of the photocatalyst. When two reactants competitively adsorb on the same catalyst active sites, but with different adsorption and desorption rate constants, and undergoes reaction to yield different products, the reaction could be represented by the Langmuir-Hinshelwood (L-H) mechanism [53, 54, 61-65]. Hence, the L-H model was employed to correlate the as-obtained experimental data. Multiple variable, non-linear regression was carried out to determine the kinetic parameters such as reaction rate constant and adsorption equilibrium constants. The present work also aimed to extend the fundamental understanding of possible mechanism of CO_2 photoreduction over GO-OTiO_2 under visible light irradiation.

2. Experimental

2.1 Chemicals

Graphite powder (< 45 micron, > 99.99%), phosphorus pentoxide, P_2O_5 (• 98.0%), potassium persulfate, $K_2S_2O_8$ (• 99.0%), potassium permanganate, $KMnO_4$ (• 99.0%), titanium (IV) butoxide, TBOT (97.0%), ethylene glycol, EG (• 99.0%), acetic acid, HAc (• 99.7%), Degussa P25 (21 nm particle size, • 99.5%) and anatase TiO_2 (< 25 nm particle size, 99.7%) were supplied by Sigma Aldrich. Hydrogen peroxide, H_2O_2 (30.0%) and concentrated sulfuric acid, H_2SO_4 (95-97%) were supplied by Chemolab. Hydrochloric acid, HCl (37% diluted to 10%) was supplied

by Merck. All chemicals were of analytical reagent grade and were used as received without further purification. Deionized water (DI-H_2O) was used in all experiments.

2.2 Preparation of oxygen-rich TiO_2 (O_2-TiO_2) and graphene oxide/oxygen-rich TiO_2 (GO-$OTiO_2$) hybrid composite.

The fabrication of O_2-TiO_2 and GO-$OTiO_2$ has been reported in our previous work [10, 47, 48]. In brief, TBOT was added dropwise into pre-chilled DI-H_2O, which resulted in an immediate precipitation of hydrolyzed titanium species. The solution was filtered and subsequently washed with 1 L of DI-H_2O, after which the precipitate was added into a mixture consisting of 100 mL DI-H_2O and 80 mL H_2O_2. The resulting orange colored peroxo-titanate complex was heated at 50 ^{o}C for 3 h, and then dried in an air oven at 100 ^{o}C overnight. The yellowish solid material was then calcined in air at 300 ^{o}C for 2 h with a temperature ramping rate of 10 ^{o}C/min. GO was incorporated with O_2-TiO_2 *via* a wet chemical impregnation method. To attain GO sheets, graphite oxide powder was first synthesized using a modified Hummers' Method [66], followed by ultrasonication for 1.5 h to exfoliate and separate the graphitic layers. A pre-calculated amount of O_2-TiO_2 powder was introduced into the GO aqueous solution and stirred for 1 h. The solution was heated to 80 ^{o}C for 2 h, and then dried in an air oven overnight before use. Based on our previous work [10], it was observed that GO-$OTiO_2$ with a GO loading of 5 wt. % (5GO-$OTiO_2$) gave the optimum performance towards CO_2 photoreduction. Hence, the aforementioned photocatalyst was used throughout the present work.

2.3 Photocatalytic reduction of CO_2

The schematic photocatalytic reaction system for the reduction of CO_2 with H_2O in gaseous phase is shown in Fig. 1. The homemade photocatalytic system consisted of three quartz columns

connected in series, which were enclosed within a black box to avoid any interference from the surrounding light. The dimensions of the quartz columns are as follows: inner diameter = 9 mm, outer diameter = 11 mm, length = 250 mm. The entire system was checked for any leakages using a soap bubble solution. Process and kinetic studies of the CO_2 photoreduction process were conducted over 5GO-OTiO_2 photocatalyst. The sample was coated onto glass rods using double-sided tape, which were then loaded into the quartz columns. The photoreduction experiments were conducted at ambient condition (25 ± 5 ^{o}C, 1 bar) in a continuous gas flow reactor. A xenon arc lamp (Model no: CHF XM500W) with a UV cut-off filter ($>$ 400 nm) was employed throughout the study to focus the photocatalytic experiments solely on visible light irradiation. The average irradiance and light spectrum of the xenon lamp were recorded by an Avantes fiber optic spectrometer (AvaSpec-128) equipped with a cosine corrector. The required data was obtained using the AvaSoft-8 software. Before taking any measurements, an irradiance calibration was first carried out using the AvaLight-HAL-CAL light source. As an additional experiment, the photoreduction of CO_2 at optimized process conditions were repeated under the air mass 1.5 (AM1.5) filter. The light spectrums of the xenon arc lamp equipped with UV cut-off filter and the AM1.5 filter are shown in the Supplementary Material.

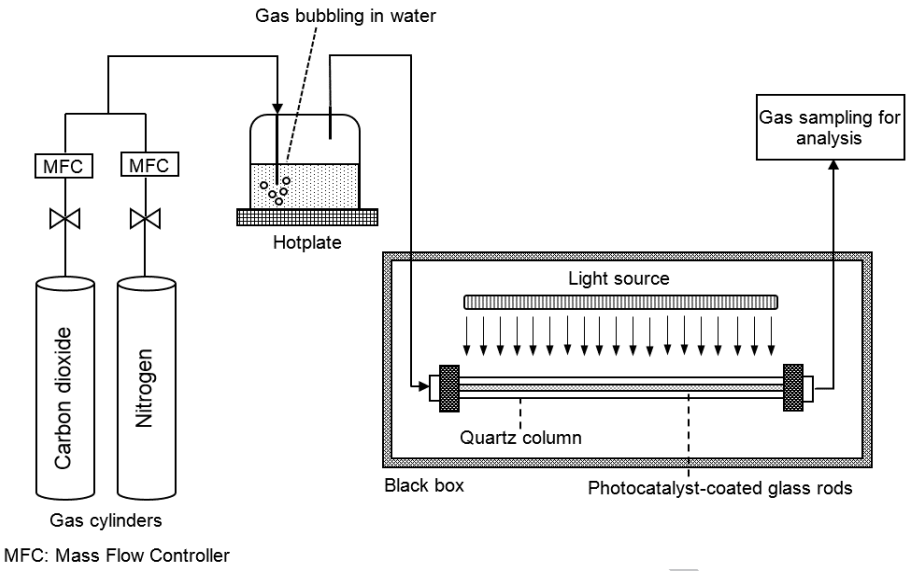

Fig. 1. Schematic of the apparatus used for the photocatalytic reduction of CO_2 under visible light irradiation.

After loading the photocatalyst-coated glass rods, highly pure CO_2 (99.99%) was bubbled through water to produce a mixture of CO_2 and water vapour into the photoreactor at atmospheric pressure. Before switching on the light source, wet CO_2 was permitted to flow through the photoreactor at 30 ml/min for 30 min to eliminate any excess air and to ensure the complete adsorption of gas molecules. After purging the reactor with wet CO_2, the xenon lamp was switched on and the flow of CO_2/H_2O was regulated using a mass flow controller. The temperature in the reactor was closely monitored with a thermocouple attached to a digital temperature reader. The distance between the light source and the photoreactor was measured to be about 5 cm. An "online" gas chromatography (GC) system (Agilent 7820A) coupled with flame ionization detector (FID) and thermal conductivity detector (TCD) was used to analyze the composition of the product gas. Throughout the fixed duration of 8 h, the product gas was collected and analyzed downstream of the reactor at 0.5 h intervals.

The process parameters studied in this work included the intensity of the incident light source as well as the partial pressures of both CO_2 and water vapour. To vary the intensity of the incident light, the electric current of the xenon arc lamp was manipulated in the range of 5 – 15 A, where the irradiance (mW/cm^2) at each setting was recorded (see Supplementary Material). The partial pressure of CO_2, P_{CO_2} used in the photocatalytic experiment was varied in the range of 25 – 101 kPa, which was achieved by controlling the flow ratio of CO_2 to the inert gas N_2. The total flow rate entering the photoreactor was held constant at 5 ml/min throughout the duration of all experiments. Finally, the partial pressure of H_2O, P_{H_2O} or moisture content entering the photoreactor was varied by controlling the temperature of the water saturator.

3. Results and Discussion

3.1 Effects of process parameters on the photoreduction of CO_2 under visible light irradiation

Initially, a series of control experiments were performed to confirm that the hydrocarbon products were generated through photocatalytic reaction rather than through organic decomposition of the 5GO-OTiO_2 photocatalyst. The control experiments were conducted under the following conditions: (1) in the dark (without light irradiation) with the presence of photocatalyst and CO_2/H_2O flow, (2) without photocatalyst under CO_2/H_2O flow and light irradiation, (3) in the absence of H_2O vapor with photocatalyst, CO_2 flow and light irradiation and (4) under N_2/H_2O atmosphere in the presence of photocatalyst and light irradiation. In all cases, no appreciable product formation could be detected. This confirmed that the evolved products were generated through the photocatalytic process and not from the photodecomposition of organic residues on the catalyst. Therefore, it can be reiterated that the

CO_2 photoreduction process required all three components, *i.e.* the presence of photocatalysts, reactant feed (CO_2 and H_2O) and light irradiation.

The intensity of the light source was varied between 65.3 – 177.2 mW/cm^2 (see Supplementary Material). The CO_2 photoreduction experiments were conducted at a fixed CO_2 flowrate of 5 ml/min at ambient condition. The temperature of the photocatalytic system was closely monitored throughout the duration of the reaction. Despite the high intensity of the xenon arc lamp used in the experiments, the temperature increase was observed to be minimal and insignificant. Fig. 2(a) shows the total CH_4 yield versus light intensity under fixed CO_2 and H_2O pressures of 101 and 4.33 kPa, respectively. The total CH_4 yield attained was promoted almost linearly with the incident light intensity. At an intensity of 177.2 mW/cm^2, the highest total CH_4 yield of 3.14 μmol g_{cat}^{-1} was achieved after 8 h of light irradiation. This observation could be attributed to the large number of photons striking the surface of the 5GO-OTiO$_2$ photocatalyst, which in turn powered the excitation of more electrons and holes to take part in the photoreduction of CO_2 into CH_4 gas [67-69].

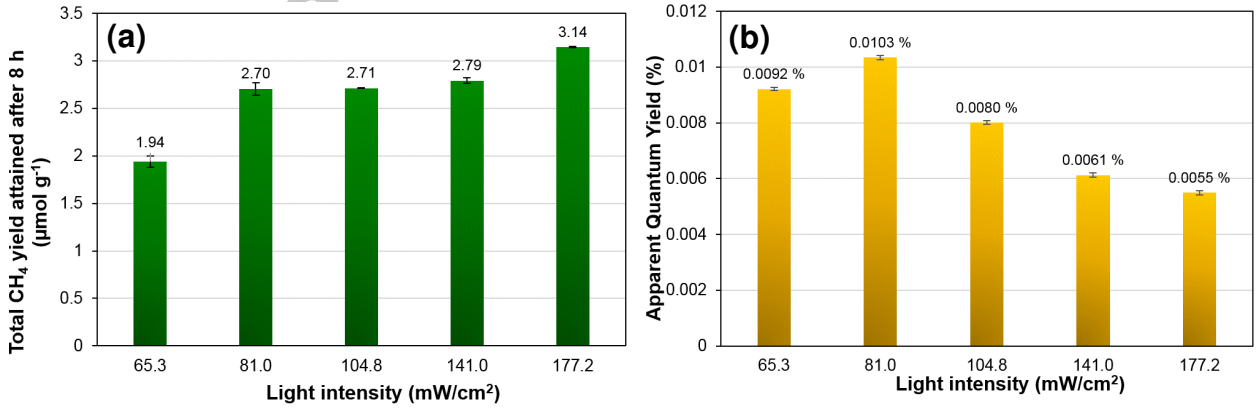

Fig. 2. (a) Total methane yield and (b) apparent quantum yield attained over 5GO-OTiO$_2$ after 8 h at different light intensities, P_{CO_2} : 101 kPa; P_{H_2O} : 4.33 kPa.

Although the photocatalytic performance of a sample is typically measured by the product yield attained in terms of μmol g_{cat}^{-1} or μmol $g_{cat}^{-1} h^{-1}$, it should be noted that the photocatalytic activity is generally dependent on other factors such as the intensity of the light source employed. Therefore, to determine the optimum light intensity for this process, the apparent quantum yield (AQY) was adopted. AQY is defined as the ratio of the number of electrons reacted to the number of incident photons at that time period. The general equation is described by Eq. (1). In the photocatalytic reduction of CO_2 into CH_4 gas, eight electrons are consumed per formation of one CH_4 molecule as described by Eq. (2). Hence, the number of electrons reacted can be directly calculated by multiplying the number of CH_4 molecules evolved by eight. As a result, the AQY can be estimated by Eq. (3) [49, 70].

$$\text{Apparent quantum yield}(\%) = \frac{\text{Number of reacted electrons}}{\text{Number of incident photons}} \text{ x } 100\% \quad (1)$$

$$CO_2 + 8H^+ + 8e^- \rightarrow CH_4 + 2H_2O \quad (2)$$

$$\text{Apparent quantum yield}(\%) = \frac{[CH_4] \times 8 \times N_A}{H \text{ x } A \times \frac{\lambda}{hc} \times t} \times 100\% \quad (3)$$

Where $[CH_4]$ represents the amount of CH_4 evolved during the photoreaction (mol), N_A is the Avogadro's number (mol^{-1}), H is the apparent light intensity used (W m^{-2}), A is the irradiation area (m^2), λ is the light wavelength (m), h is the Planck's constant (J s), c is the speed of light (m s^{-1}) and t is the reaction time (s).

The AQY obtained over 5GO-OTiO_2 photocatalyst at different light intensities are shown in Fig. 2(b). Among the studied incident light intensities, 5GO-OTiO_2 was observed to exhibit the highest AQY of 0.0103% at an intensity of 81.0 mW/cm^2. An optimum value existed because at

excessively high light intensities (> 81 mW/cm^2), the photons supplied to the photocatalyst would have exceeded the number of photons required for the photocatalytic reaction. Therefore, an irradiance of 81 mW/cm^2 gave the most efficient utilization of photon energy and was hence used in all subsequent studies.

The influence of CO_2 partial pressure on the photocatalytic activity was also investigated. As the present work focuses mainly on the production of hydrocarbon fuels, the representation of photocatalytic efficiency was directed towards the total yield of CH_4 product. Fig. 3(a) shows the total CH_4 yields attained over 5GO-OTiO$_2$ after 8 h versus different CO_2 pressures under fixed light intensity, 81 mW/cm^2 and water pressure, 4.33 kPa at room temperature. From Fig. 3(a), it can be observed that the total yield of CH_4 increased with P_{CO_2}, where it reached a maximum value of 3.08 μmol g_{cat}^{-1} at 90 kPa, before decreasing with a further increment of P_{CO_2}. This phenomenon was likely due to the competitive adsorption between CO_2 and H_2O molecules on the active sites of 5GO-OTiO$_2$ during the photoreduction process. At lower concentrations of CO_2, a large amount of H_2O molecules could have adsorbed on the photocatalyst surface to react with a limited number of CO_2 molecules to form CH_4. On the other hand, at excessively high CO_2 concentrations, the CO_2 molecules would compete with H_2O molecules for the active sites, leading to poor overall photoactivity [61, 65, 71]. Therefore, an optimum concentration of both reactants exists for achieving high CH_4 yield. A similar trend of results have also been reported by other research groups [57, 61, 65].

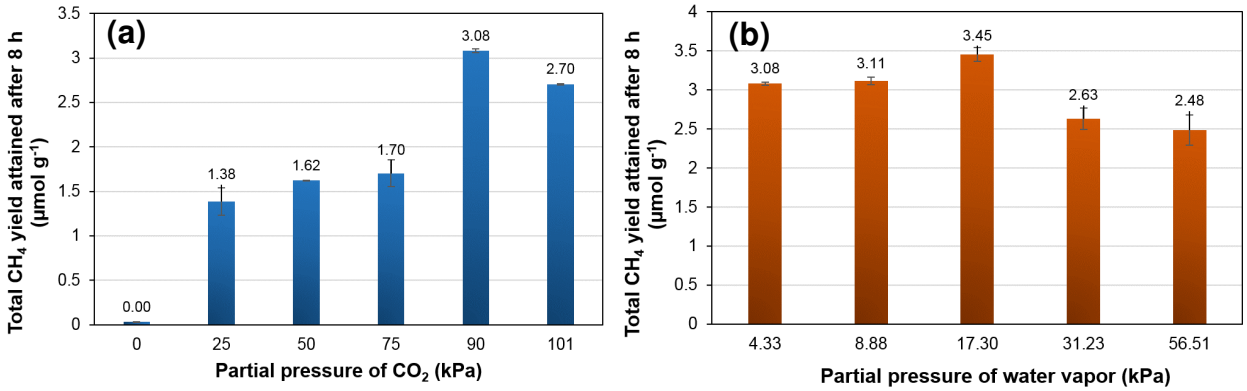

Fig. 3. Total methane yield attained over 5GO-OTiO$_2$ after 8 h at (a) different partial pressures of CO_2, light intensity: 81.0 mW/cm^2; P_{H_2O}: 4.33 kPa; and at (b) different partial pressures of H_2O, light intensity: 81.0 mW/cm^2; P_{CO_2} : 90 kPa.

Fig. 3(b) illustrates the effect of H_2O partial pressure on the photocatalytic activity of 5GO-OTiO$_2$, under fixed light intensity and CO_2 pressure of 81 mW/cm^2 and 90 kPa, respectively. From Fig. 3(b), the total CH_4 yield can be seen to have increased with P_{H_2O} until reaching a maximum value of 3.45 μmol g_{cat}^{-1} at 17.3 kPa. Increasing the P_{H_2O} further was found to have a negative impact on the photocatalytic performance of 5GO-OTiO$_2$. Similar to the case of P_{CO_2}, this phenomenon implied a competitive adsorption of reactants, *i.e.* CO_2 and H_2O for the active sites during the photoreduction process [61]. The presence of water vapour in the CO_2 photoreduction process is indispensable due to its role in producing certain reactive intermediate radicals. During the photocatalytic reduction of CO_2, the photogenerated holes (h^+) react with H_2O to yield H^+ ions and •OH radicals, both of which are required for the subsequent reduction of CO_2. The •H radicals which originate from the reduction of protons, will react with carbon radicals on the photocatalyst surface to produce methyl radicals, *i.e.* •CH_2, •CH_3 and finally CH_4 as well as higher hydrocarbons *e.g.* C_2H_4 and C_2H_6 [53, 57, 72]. Therefore, H_2O is needed in appropriate concentrations to ensure the sufficient supply of H^+ ions and •OH for the formation of

these hydrocarbon products. However, excessively high H_2O concentrations would occupy the catalyst active sites and consequently reduce the surface contact of CO_2 molecules with the photocatalyst.

The highest CH_4 yield of 3.45 μmol g_{cat}^{-1} could be obtained over 5GO-OTiO_2 at P_{CO_2} = 90 kPa, P_{H_2O} = 17.3 kPa under an incident visible light intensity of 81.0 mW/cm^2 after 8 h. In addition to CH_4, other products such as CO, C_2H_4 and C_2H_6 were also detected at the outlet gas (see Fig. 4). The total yield of CO evolved was found to be approximately 2.6 times higher than that of CH_4. This observation could be explained based on the energy band theory. Principally, photoexcited electrons could only be consumed effectively if the reduction potential of the reaction is lower than the CB potential of the semiconductor. In this case, the 5GO-OTiO_2 photocatalyst was more feasible in driving the reduction of CO_2 into CO because of the lower reduction potential difference of $(E^o(CO_2/CO = -0.53V)$ as compared to CH_4 $(E^o(CO_2/CH_4 = -0.24V)$ [73]. Therefore, in the continuous process, a significant amount of CO was produced.

In an additional experiment, the photocatalytic reduction of CO_2 at optimized process conditions was repeated under the air mass 1.5 (AM1.5) filter (see Fig. 4). The use of the AM1.5 provides one of the best options for simulating natural sunlight [74]. It was found that the total yield of all four products was higher under the AM1.5 filter than that of UV cut-off. This is because UV-light is generally known to exhibit higher energy per photon, which has the potential to effectively power the excitation of more electrons and holes for the photocatalytic reactions, thus leading to the increase in product yield [75]. To confirm the as-obtained results, the CO_2 photoreduction experiment conducted under the optimized process conditions were repeated. The

standard error for the formation of each product was found to be approximately ± 0.1, thus confirming the reproducibility of the results.

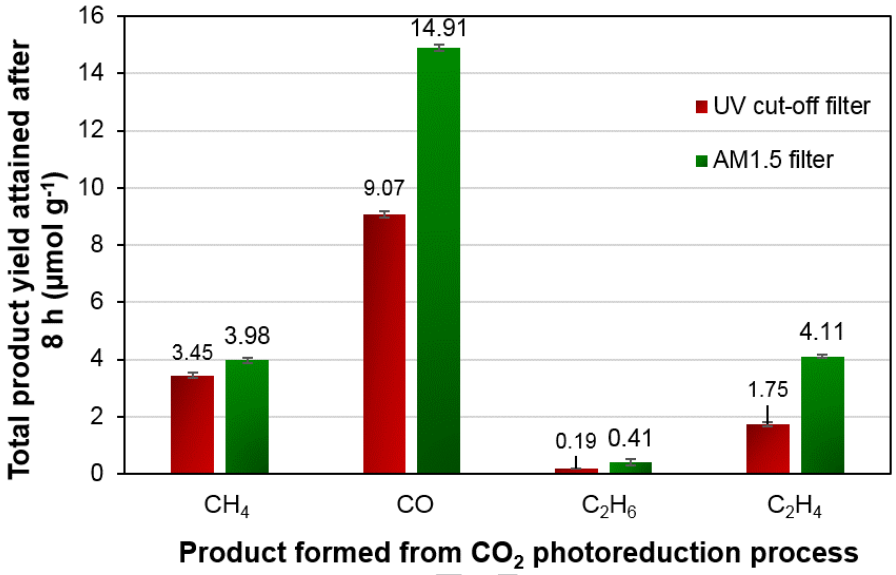

Fig. 4. Total yield of CH_4, CO, C_2H_6 and C_2H_4 attained over 5GO-OTiO_2 after 8 h under different light filters.

3.2 Kinetic study of the photocatalytic reduction of CO_2 over 5GO-OTiO_2 composite

In heterogeneous photocatalytic processes, rates are typically proportional to the adsorption of reactants with efficient desorption of products on the photocatalyst surface. When two reactants competitively adsorb on the same catalyst surface active sites, but with different adsorption and desorption constants, the reaction can be represented using the Langmuir-Hinshelwood mechanism [76], as described by Eq. (4).

$$\text{Rate} = \mathrm{k}\theta_A\theta_B = \mathrm{k}\frac{K_A P_A K_B P_B}{(1+K_A P_A + K_B P_B)^2} \quad (4)$$

Where θ_A and θ_B represent the fractional surface coverage of each reactant, while P_A and P_B are the partial pressures of each reactant species. The rate constant, k and adsorption equilibrium constants, K_A and K_B, are dependent on the system temperature. If the adsorption is random, the adsorption probability would be taken as the fraction of the uncovered surface (1 - θ), while desorption would be taken as the surface covered, θ. By employing these assumptions, the kinetic model for the photocatalytic reduction of CO_2 with H_2O could be developed. In the photoreduction process, CO_2 and H_2O were photocatalytically converted into CH_4 and CO as main products through Eq. (5).

$$3CO_2 + 2H_2O \xrightarrow{h\nu} CH_4 + 2CO + 3O_2 \quad (5)$$

There are five primary steps in the photocatalytic reaction mechanism. Step 1 is the adsorption of reactants, *i.e.* CO_2 and H_2O onto the active sites of 5GO-OTiO_2; Step 2 consists of light absorption and subsequent production of photoinduced electrons and holes on the photocatalyst surface; Step 3 is the interaction between the charge carriers and adsorbed reactant molecules, as well as the recombination of charge particles; Step 4 consists of both the oxidation and reduction reactions while the last step is the desorption of products from the photocatalyst surface [53, 65]. Among the aforementioned steps, the surface reaction is typically considered to be the slowest and hence the rate determining step (RDS) [53, 54]. By assuming the reactants and products are adsorbed on the same catalyst surface active sites, the rate of reaction in the CO_2 photoreduction process can be explained by the Langmuir-Hinshelwood mechanism as described in Eq. (6).

$$\text{Rate} = \left(kI^a\right)\left(\frac{K_{H_2O}P_{H_2O}K_{CO_2}P_{CO_2}}{(1+K_{H_2O}P_{H_2O}+K_{CO_2}P_{CO_2}+K_{CO}P_{CO}+K_{O_2}P_{O_2}+K_{CH_4}P_{CH_4})^2}\right) \quad (6)$$

Where k represents the rate constant of any particular product and I is the incident light intensity in which the kinetic constants are evaluated. Generally, the photocatalytic reaction rate is proportional to I^a, where *a* is the reaction order of the light intensity. K_{H_2O}, K_{CO_2}, K_{CO}, K_{O_2} and K_{CH_4} are the ratios of rate constants for adsorption and desorption of H_2O, CO_2, CO, O_2 and CH_4, respectively. By assuming that only reactants are adsorbed onto the photocatalyst surface while all products desorbed immediately after chemical reaction, Eq. (6) can be further simplified to Eq. (7). In addition, the reaction was considered to be irreversible because the partial pressures of the products were very low [61].

$$\text{Rate} = \left(kI^a K_{H_2O} K_{CO_2}\right)\left(\frac{P_{H_2O} P_{CO_2}}{(1 + K_{H_2O} P_{H_2O} + K_{CO_2} P_{CO_2})^2}\right) \quad (7)$$

The constants of the L-H model were solved by correlating it with the experimental data of P_{CO_2}, P_{H_2O}, light intensity and the CH_4 production rate obtained from Section 3.1, where the light intensity, *I* was fixed at the optimum value of 81.0 mW/cm^2. Multiple-variable non-linear regression was performed using Polymath software, version 6.10. The best fitted rate constant, k, adsorption equilibrium constants, K_{H_2O} and K_{CO_2} as well as the reaction order of the light intensity, *a* are tabulated in Table 1. The fitted model showed high degree of precision, exhibiting an R-squared value of 0.922 with small sums of squares/ variance. By incorporating the values of the kinetic constants, the resulting rate model for the photocatalytic reduction of CO_2 over 5GO-OTiO_2 is presented in Eq. (8).

Table 1. Adsorption equilibrium and rate constants of Langmuir-Hinshelwood model estimated using experimental data on 5GO-OTiO$_2$.

Parameter	**Value**	**Error with 95% confidence**
Reaction rate constant, k (μmol $g_{cat}^{-1} h^{-1}$)	84.42	± 0.267
Reaction order of light intensity, *a*	0.044	± 0.0007
Adsorption equilibrium of H_2O, K_{H_2O} (bar^{-1})	8.070	± 0.0620
Adsorption equilibrium of CO_2, K_{CO_2} (bar^{-1})	0.0193	± 0.0001

$$\text{Rate}=15.953\left(\frac{P_{H_2O}P_{CO_2}}{(1+8.070\,P_{H_2O}+0.0193\,P_{CO_2})^2}\right) \quad (8)$$

Based on the tabulated data in Table 1, the value of H_2O adsorption equilibrium, K_{H_2O} was 8.07 bar^{-1}, which was significantly higher than that of CO_2 (K_{CO_2} = 0.02 bar^{-1}). The value of K_{CO_2} was near zero, which directly indicated very weak adsorption of CO_2 molecules, while water was strongly adsorbed on the surface of the 5GO-OTiO$_2$ photocatalyst. This is because, in addition to the strong hydrophilic nature of graphene oxide [77, 78]. it is well known that the surface of TiO_2

becomes superhydrophilic when irradiated by light [79]. Therefore, water would wet most of the surface of 5GO-OTiO$_2$ during the photocatalytic process. As shown in Table 1, the power of the light intensity was estimated to be approximately 0.044 in the CH_4 rate equation. As discussed earlier, photocatalytic activity is generally directly proportional to the light intensity. However, if the supply of light flux exceeds the demand for the photoreaction, the power of light intensity in the rate equation would gradually shift from one to less than 0.5. Therefore, it can be deduced that the light flux used in our experiments was probably over-supplied and can be decreased to enhance the quantum efficiency of the photocatalytic system. To prove the validity of the rate model in Eq. (8), the CO_2 photoreduction experiments were repeated and the production rate of CH_4 were compared to that obtained from the rate model. The curves representing the profiles of CH_4 production rate as a function of P_{H_2O} and P_{CO_2} using the kinetic model is shown in the Supplementary Material. The model was shown to have fitted well to the experimental data using the constants as summarized in Table 1, with R^2 values above 0.95.

Although the detailed mechanism underlying the formation of CH_4 could not be determined in the present study, a CO_2 photoreduction mechanism is suggested based on the L-H model derived and is illustrated in Fig. 5. The photocatalytic process begins with the adsorption of reactant molecules, *i.e.* CO_2 and H_2O molecules onto the surface of 5GO-OTiO$_2$. In the surface reaction step, photogenerated electrons are transferred to the adsorbed CO_2 to yield $\bullet CO_2^-$ radicals. The holes, on the other hand, react with adsorbed H_2O molecules to produce H^+ ions and •OH radicals, and subsequently O_2 [80]. The •H radicals formed through the reduction of proton then react with carbon radicals on the photocatalyst surface to yield intermediate radicals and the hydrocarbon products. All possible reaction steps which take place in the photocatalytic reduction of CO_2 with

H_2O are explained by Eq. (9 – 13). Desorption of the evolved products represents the final step in the photocatalytic process.

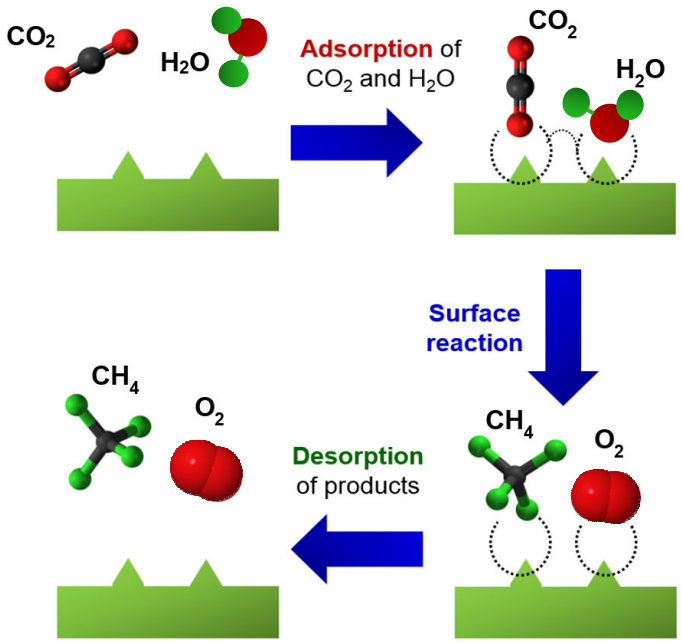

Fig. 5. Conceptual diagram depicting the reaction mechanism of the CO_2 photoreduction process based on the Langmuir-Hinshelwood mechanism.

$$H_2O + h^+ \rightarrow \bullet OH + H^+ \xrightarrow{e,\, H_2O} \bullet 4H + O_2 \quad (9)$$

$$CO_2 + e^- \xrightarrow{\bullet H} \bullet CO_2^- \rightarrow CO + OH^- \quad (10)$$

$$CO + e^- \rightarrow \quad (11)$$

$$\bullet C + \bullet H \rightarrow \bullet CH \xrightarrow{\bullet H} \bullet CH_2 \xrightarrow{\bullet H} \bullet CH_3 \xrightarrow{\bullet H} CH_4 \quad (12)$$

$$n \bullet CH_2 + m \bullet CH_3 \xrightarrow{\bullet H} C_2H_4 + C_2H_6 \quad (13)$$

4. Conclusions

In summary, process parameters including radiant flux intensity and the partial pressures of both CO_2 and water vapour were systematically varied and studied in order to study their effects on the CO_2 photoreduction process over 5GO-OTiO_2 photocatalyst. The visible light irradiance was varied between 65.3 to 177.2 mW/cm^2 to study its effect on the apparent quantum yield (AQY) of 5GO-OTiO_2. It was found that the optimum irradiance for the process was 80.97 mW/cm^2. Beyond that value, the AQY was shown to have gradually decreased. This was because the photons generated at excessively high light intensities have exceeded the number of photons required for the photocatalytic reaction. The partial pressure of CO_2 and water vapour which gave the highest yield of CH_4 gas was found to be 90 kPa and 17.3 kPa, respectively. The combination of these process parameters resulted in a total CH_4 yield of 3.450 μmol g_{cat}^{-1} after 8 h of reaction time. The experimental data obtained was then fitted into the Langmuir-Hinshelwood surface reaction mechanism, wherein both CO_2 and H_2O adsorbed simultaneously on the photocatalyst surface to form the CH_4 product. Through regression fitting, the reaction rate as well as CO_2 and H_2O adsorption equilibrium constants were determined to be 84.42 μmol $g_{cat}^{-1} h^{-1}$, 0.019 bar^{-1} and 8.07 bar^{-1}, respectively. The significantly smaller CO_2 adsorption equilibrium constant implied that the adsorption of CO_2 was very weak while water strongly adsorbed on the photocatalyst surface. The fitted model showed high degree of precision, exhibiting an R-squared value of 0.95.

Acknowledgements

This work was funded by the Ministry of Science, Technology and Innovation (MOSTI) Malaysia and the Ministry of Higher Education (MOHE) under e-Science Fund (Ref.

no. 03-02-10-SF0244) and the Fundamental Research Grant Scheme (FRGS) (Ref. no. FRGS/1/2013/TK05/MUSM/02/1), respectively.

References

[1] S.I. Seneviratne, M.G. Donat, A.J. Pitman, R. Knutti, R.L. Wilby, Allowable CO_2 emissions based on regional and impact-related climate targets, Nature 529 (2016) 477-483.

[2] M. Forkel, N. Carvalhais, C. Rödenbeck, R. Keeling, M. Heimann, K. Thonicke, S. Zaehle, M. Reichstein, Enhanced seasonal CO_2 exchange caused by amplified plant productivity in northern ecosystems, Science DOI: 10.1126/science.aac4971 (2016).

[3] J. Chang, P. Ciais, N. Viovy, N. Vuichard, M. Herrero, P. Havlík, X. Wang, B. Sultan, J.-F. Soussana, Effect of climate change, CO_2 trends, nitrogen addition, and land-cover and management intensity changes on the carbon balance of European grasslands, Global Change Biology 22 (2016) 338-350.

[4] H. Kashiwagi, Atmospheric carbon dioxide and climate change since the Late Jurassic (150 Ma) derived from a global carbon cycle model, Palaeogeography, Palaeoclimatology, Palaeoecology 454 (2016) 82-90.

[5] Y. Hao, H. Chen, Y.-M. Wei, Y.-M. Li, The influence of climate change on CO_2 (carbon dioxide) emissions : an empirical estimation based on Chinese provincial panel data, J. Clean. Prod. DOI: 10.1016/j.jclepro.2016.04.117.

[6] A. Sarkar, E. Gracia-Espino, T. Wågberg, A. Shchukarev, M. Mohl, A.-R. Rautio, O. Pitkänen, T. Sharifi, K. Kordas, J.-P. Mikkola, Photocatalytic reduction of CO_2 with H_2O over modified TiO_2 nanofibers: Understanding the reduction pathway, Nano Res. DOI: 10.1007/s12274-016-1087-9 (2016) 1-13.

[7] J.-C. Wang, H.-C. Yao, Z.-Y. Fan, L. Zhang, J.-S. Wang, S.-Q. Zang, Z.-J. Li, Indirect Z-Scheme BiOI/g-C_3N_4 photocatalysts with enhanced photoreduction CO_2 activity under visible light irradiation, ACS Appl. Mater. Interfaces 8 (2016) 3765-3775.

[8] X. Chang, T. Wang, J. Gong, CO_2 photo-reduction: insights into CO_2 activation and reaction on surfaces of photocatalysts, Energy Environ. Sci. DOI: 10.1039/C6EE00383D (2016).

[9] B. Yu, Y. Zhou, P. Li, W. Tu, P. Li, L. Tang, J. Ye, Z. Zou, Photocatalytic reduction of CO_2 over Ag/TiO_2 nanocomposites prepared with a simple and rapid silver mirror method, Nanoscale DOI: 10.1039/C6NR02547A (2016).

[10] L.-L. Tan, W.-J. Ong, S.-P. Chai, B.T. Goh, A.R. Mohamed, Visible-light-active oxygen-rich TiO_2 decorated 2D graphene oxide with enhanced photocatalytic activity toward carbon dioxide reduction, Appl. Catal., B 179 (2015) 160-170.

[11] L.-L. Tan, W.-J. Ong, S.-P. Chai, A.R. Mohamed, Reduced graphene oxide-TiO_2 nanocomposite as a promising visible-light-active photocatalyst for the conversion of carbon dioxide, Nanoscale Res. Lett. 8 (2013) 465-473.

[12] L.-L. Tan, W.-J. Ong, S.-P. Chai, A.R. Mohamed, Noble metal modified reduced graphene oxide/TiO_2 ternary nanostructures for efficient visible-light-driven photoreduction of carbon dioxide into methane, Appl. Catal., B 166–167 (2015) 251-259.

[13] W.-J. Ong, L.-L. Tan, S.-P. Chai, S.-T. Yong, A.R. Mohamed, Surface charge modification via protonation of graphitic carbon nitride (g-C_3N_4) for electrostatic self-assembly construction of 2D/2D reduced graphene oxide (rGO)/g-C_3N_4 nanostructures toward enhanced photocatalytic reduction of carbon dioxide to methane, Nano Energy 13 (2015) 757-770.

[14] H.-Q. Xu, J. Hu, D. Wang, Z. Li, Q. Zhang, Y. Luo, S.-H. Yu, H.-L. Jiang, Visible-light photoreduction of CO_2 in a metal–organic framework: Boosting electron–hole separation via electron trap states, J. Am. Chem. Soc. 137 (2015) 13440-13443.

[15] M.-Q. Yang, N. Zhang, M. Pagliaro, Y.-J. Xu, Artificial photosynthesis over graphene-semiconductor composites. Are we getting better?, Chem. Soc. Rev. 43 (2014) 8240-8254.

[16] W.-J. Ong, L.-L. Tan, Y.H. Ng, S.-T. Yong, S.-P. Chai, Graphitic carbon nitride (g-C_3N_4)-based photocatalysts for artificial photosynthesis and environmental remediation: Are we a step closer to achieving sustainability?, Chem. Rev. DOI: 10.1021/acs.chemrev.6b00075 (2016).

[17] L.K. Putri, L.-L. Tan, W.-J. Ong, W.S. Chang, S.-P. Chai, Graphene oxide: Exploiting its unique properties toward visible-light-driven photocatalysis, Appl. Mater. Today 4 (2016) 9-16.

[18] O. Ola, M.M. Maroto-Valer, Review of material design and reactor engineering on TiO_2 photocatalysis for CO_2 reduction, J. Photochem. Photobiol., C 24 (2015) 16-42.

[19] P. Zhou, J. Yu, M. Jaroniec, All-solid-state Z-scheme photocatalytic systems, Adv. Mater. 26 (2014) 4920-4935.

[20] A.D. Handoko, K. Li, J. Tang, Recent progress in artificial photosynthesis: CO_2 photoreduction to valuable chemicals in a heterogeneous system, Curr. Opin. Chem. Eng. 2 (2013) 200-206.

[21] K. Li, X. An, K.H. Park, M. Khraisheh, J. Tang, A critical review of CO_2 photoconversion: Catalysts and reactors, Catal. Today 224 (2014) 3-12.

[22] J.L. White, M.F. Baruch, J.E. Pander Iii, Y. Hu, I.C. Fortmeyer, J.E. Park, T. Zhang, K. Liao, J. Gu, Y. Yan, T.W. Shaw, E. Abelev, A.B. Bocarsly, Light-driven heterogeneous

reduction of carbon dioxide: Photocatalysts and photoelectrodes, Chem. Rev. 115 (2015) 12888-12935.

[23] W.-J. Ong, L.-L. Tan, S.-P. Chai, S.-T. Yong, A.R. Mohamed, Highly reactive {001} facets of TiO_2-based composites: synthesis, formation mechanism and characterization, Nanoscale 6 (2014) 1946-2008.

[24] W.-J. Ong, L.-L. Tan, S.-P. Chai, S.-T. Yong, A.R. Mohamed, Facet-dependent photocatalytic properties of TiO_2-based composites for energy conversion and environmental remediation, ChemSusChem 7 (2014) 690-719.

[25] P. Pichat, Fundamentals of TiO_2 Photocatalysis. Consequences for Some Environmental Applications, in: C.J. Colmenares, Y.-J. Xu (Eds.) Heterogeneous Photocatalysis: From Fundamentals to Green Applications, Springer Berlin Heidelberg, Berlin, Heidelberg, 2016, pp. 321-359.

[26] C. Peng, X. Yang, Y. Li, H. Yu, H. Wang, F. Peng, Hybrids of two-dimensional Ti_3C_2 and TiO_2 Exposing {001} facets toward enhanced photocatalytic activity, ACS Appl. Mater. Interfaces 8 (2016) 6051-6060.

[27] G. Peng, J.E. Ellis, G. Xu, X. Xu, A. Star, In situ grown TiO_2 nanospindles facilitate the formation of holey reduced graphene oxide by photodegradation, ACS Appl. Mater. Interfaces 8 (2016) 7403-7410.

[28] X. Liu, G. Dong, S. Li, G. Lu, Y. Bi, Direct observation of charge separation on anatase TiO_2 crystals with selectively etched {001} facets, J. Am. Chem. Soc. 138 (2016) 2917-2920.

[29] S.J. Pearton, C.R. Abernathy, M.E. Overberg, G.T. Thaler, D.P. Norton, N. Theodoropoulou, A.F. Hebard, Y.D. Park, F. Ren, J. Kim, L.A. Boatner, Wide band gap ferromagnetic semiconductors and oxides, J. Appl. Phys. 93 (2003) 1-13.

[30] N. Serpone, Is the band gap of pristine TiO_2 narrowed by anion- and cation-doping of titanium dioxide in second-generation photocatalysts?, J. Phys. Chem. B 110 (2006) 24287-24293.

[31] S. Mubeen, G. Hernandez-Sosa, D. Moses, J. Lee, M. Moskovits, Plasmonic photosensitization of a wide band gap semiconductor: Converting plasmons to charge carriers, Nano Lett. 11 (2011) 5548-5552.

[32] J.B. Varley, A. Janotti, C. Franchini, C.G. Van de Walle, Role of self-trapping in luminescence and p-type conductivity of wide-band-gap oxides, Phys. Rev. B 85 (2012) 081109.

[33] H. Yan, X. Wang, M. Yao, X. Yao, Band structure design of semiconductors for enhanced photocatalytic activity: The case of TiO_2, Progress in Natural Science: Materials International 23 (2013) 402-407.

[34] D. Zhao, C. Chen, Y. Wang, H. Ji, W. Ma, L. Zang, J. Zhao, Surface modification of TiO_2 by phosphate:• Effect on photocatalytic activity and mechanism implication, J. Phys. Chem. C 112 (2008) 5993-6001.

[35] M.G. Méndez-Medrano, E. Kowalska, A. Lehoux, A. Herissan, B. Ohtani, D. Bahena, V. Briois, C. Colbeau-Justin, J.L. Rodríguez-López, H. Remita, Surface modification of TiO_2 with Ag nanoparticles and CuO nanoclusters for application in photocatalysis, J. Phys. Chem. C 120 (2016) 5143-5154.

[36] M. Epifani, R. Díaz, C. Force, E. Comini, M. Manzanares, T. Andreu, A. Genç, J. Arbiol, P. Siciliano, G. Faglia, J.R. Morante, Surface modification of TiO_2 nanocrystals by WOx coating or wrapping: Solvothermal synthesis and enhanced surface chemistry, ACS Appl. Mater. Interfaces 7 (2015) 6898-6908.

[37] W. Alammari, M. Govindhan, A. Chen, Modification of TiO_2 nanotubes with PtRu/graphene nanocomposites for enhanced oxygen reduction reaction, ChemElectroChem 2 (2015) 2041-2047.

[38] H. Choi, D. Shin, B.C. Yeo, T. Song, S.S. Han, N. Park, S. Kim, Simultaneously controllable doping sites and the activity of a W–N codoped TiO_2 photocatalyst, ACS Catal. 6 (2016) 2745-2753.

[39] M. Nolan, A. Iwaszuk, A.K. Lucid, J.J. Carey, M. Fronzi, Design of novel visible light active photocatalyst materials: Surface modified TiO_2, Adv. Mater. DOI: 10.1002/adma.201504894 (2016) n/a-n/a.

[40] J. Ni, S. Fu, C. Wu, J. Maier, Y. Yu, L. Li, Self-supported nanotube arrays of sulfur-doped TiO2 enabling ultrastable and robust sodium storage, Adv. Mater. 28 (2016) 2259-2265.

[41] S. Liu, J. Yu, Effect of F-Doping on the Photocatalytic Activity and Microstructures of Nanocrystalline TiO_2 Powders, in: H. Yamashita, H. Li (Eds.) Nanostructured Photocatalysts: Advanced Functional Materials, Springer International Publishing, Cham, 2016, pp. 187-200.

[42] F. Marco, I. Anna, L. Aoife, N. Michael, Metal oxide nanocluster-modified TiO_2 as solar activated photocatalyst materials, J. Phys.: Condens. Matter 28 (2016) 074006.

[43] S.A. Bakar, G. Byzynski, C. Ribeiro, Synergistic effect on the photocatalytic activity of N-doped TiO_2 nanorods synthesised by novel route with exposed (110) facet, J. Alloys Compd. 666 (2016) 38-49.

[44] M.R. Bayati, A.Z. Moshfegh, F. Golestani-Fard, Micro-arc oxidized S-TiO_2 nanoporous layers: Cationic or anionic doping?, Mater. Lett. 64 (2010) 2215-2218.

[45] V. Etacheri, M.K. Seery, S.J. Hinder, S.C. Pillai, Oxygen rich titania: A dopant free, high temperature stable, and visible-light active anatase photocatalyst, Adv. Funct. Mater. 21 (2011) 3744-3752.

[46] D. Pei, J. Luan, Development of visible light-responsive sensitized photocatalysts, Int. J. Photoenergy 2012 (2012) 13.

[47] L.-L. Tan, W.-J. Ong, S.-P. Chai, A.R. Mohamed, Band gap engineered, oxygen-rich TiO_2 for visible light induced photocatalytic reduction of CO_2, Chem. Commun. 50 (2014) 6923-6926.

[48] L.-L. Tan, W.-J. Ong, S.-P. Chai, A.R. Mohamed, Visible-light-activated oxygen-rich TiO_2 as next generation photocatalyst: Importance of annealing temperature on the photoactivity toward reduction of carbon dioxide, Chem. Eng. J. 283 (2016) 1254-1263.

[49] W.-J. Ong, L.-L. Tan, S.-P. Chai, S.-T. Yong, A.R. Mohamed, Self-assembly of nitrogen-doped TiO_2 with exposed {001} facets on a graphene scaffold as photo-active hybrid nanostructures for reduction of carbon dioxide to methane, Nano Res. 7 (2014) 1528-1547.

[50] L.-L. Tan, S.-P. Chai, A.R. Mohamed, Synthesis and applications of graphene-based TiO_2 photocatalysts, ChemSusChem 5 (2012) 1868-1882.

[51] Y. Ji, Y. Luo, Theoretical study on the mechanism of photoreduction of CO_2 to CH_4 on the anatase TiO_2(101) surface, ACS Catal. 6 (2016) 2018-2025.

[52] Y. Kohno, T. Tanaka, T. Funabiki, S. Yoshida, Reaction mechanism in the photoreduction of CO_2 with CH_4 over ZrO_2, Phys. Chem. Chem. Phys. 2 (2000) 5302-5307.

[53] M. Tahir, N.S. Amin, Photocatalytic reduction of carbon dioxide with water vapors over montmorillonite modified TiO_2 nanocomposites, Appl. Catal., B 142–143 (2013) 512-522.

[54] M. Tahir, N.S. Amin, Photocatalytic CO_2 reduction and kinetic study over In/TiO_2 nanoparticles supported microchannel monolith photoreactor, Appl. Catal., A 467 (2013) 483-496.

[55] K. Ko í, L. Obalová, L. Mat jová, D. Plachá, Z. Lacný, J. Jirkovský, O. Šolcová, Effect of TiO_2 particle size on the photocatalytic reduction of CO_2, Appl. Catal., B 89 (2009) 494-502.

[56] J.-C. Wang, L. Zhang, W.-X. Fang, J. Ren, Y.-Y. Li, H.-C. Yao, J.-S. Wang, Z.-J. Li, Enhanced photoreduction CO_2 activity over direct Z-Scheme -Fe_2O_3/Cu_2O heterostructures under visible light irradiation, ACS Appl. Mater. Interfaces 7 (2015) 8631-8639.

[57] I. Tseng, W.C. Chang, J. Wu, Photoreduction of CO_2 using sol–gel derived titania and titania-supported copper catalysts, Appl. Catal., B 37 (2002) 37-48.

[58] Y. Li, W.-N. Wang, Z. Zhan, M.-H. Woo, C.-Y. Wu, P. Biswas, Photocatalytic reduction of CO_2 with H_2O on mesoporous silica supported Cu/TiO_2 catalysts, Appl. Catal., B 100 (2010) 386-392.

[59] Z. Zhao, J. Fan, J. Wang, R. Li, Effect of heating temperature on photocatalytic reduction of CO_2 by N–TiO_2 nanotube catalyst, Catalysis Communications 21 (2012) 32-37.

[60] K. Ko í, K. Zatloukalova, L. Obalová, S. Krej íková, Z. Lacný, L. apek, A. Hospodková, O. Šolcová, Wavelength effect on photocatalytic reduction of CO_2 by Ag/TiO_2 catalyst, Chin. J. Catal. 32 (2011) 812-815.

[61] J.C.S. Wu, H.-M. Lin, C.-L. Lai, Photo reduction of CO_2 to methanol using optical-fiber photoreactor, Appl. Catal., A 296 (2005) 194-200.

[62] C.-C. Lo, C.-H. Hung, C.-S. Yuan, J.-F. Wu, Photoreduction of carbon dioxide with H_2 and H_2O over TiO_2 and ZrO_2 in a circulated photocatalytic reactor, Sol. Energy Mater. Sol. Cells 91 (2007) 1765-1774.

[63] T. Kentaro, T. Tsunehiro, Photocatalytic reduction of CO_2 using H_2 as reductant over solid base photocatalysts, Advances in CO_2 Conversion and Utilization, American Chemical Society2010, pp. 15-24.

[64] K. Teramura, T. Tanaka, H. Ishikawa, Y. Kohno, T. Funabiki, Photocatalytic reduction of CO_2 to CO in the presence of H_2 or CH_4 as a reductant over MgO, J. Phys. Chem. B 108 (2003) 346-354.

[65] M. Tahir, N.S. Amin, Indium-doped TiO_2 nanoparticles for photocatalytic CO_2 reduction with H_2O vapors to CH_4, Appl. Catal., B 162 (2015) 98-109.

[66] W.S. Hummers, R.E. Offeman, Preparation of graphitic oxide, J. Am. Chem. Soc. 80 (1958) 1339-1339.

[67] Y. Ku, W.-H. Lee, W.-Y. Wang, Photocatalytic reduction of carbonate in aqueous solution by UV/TiO_2 process, J. Mol. Catal. A: Chem. 212 (2004) 191-196.

[68] B.K. Sharma, R. Ameta, J. Kaur, S.C. Ameta, Photocatalytic reduction of carbon dioxide over ferrocyanide-coated titanium dioxide powder, International Journal of Energy Research 21 (1997) 923-929.

[69] W. Lin, H. Han, H. Frei, CO_2 splitting by H_2O to CO and O_2 under UV light in TiMCM-41 silicate sieve, J. Phys. Chem. B 108 (2004) 18269-18273.

[70] W.-H. Lee, C.-H. Liao, M.-F. Tsai, C.-W. Huang, J.C.S. Wu, A novel twin reactor for CO_2 photoreduction to mimic artificial photosynthesis, Appl. Catal., B 132–133 (2013) 445-451.

[71] S. Kaneco, H. Kurimoto, Y. Shimizu, K. Ohta, T. Mizuno, Photocatalytic reduction of CO_2 using TiO_2 powders in supercritical fluid CO_2, Energy 24 (1999) 21-30.

[72] M. Anpo, H. Yamashita, Y. Ichihashi, Y. Fujii, M. Honda, Photocatalytic reduction of CO_2 with H_2O on titanium oxides anchored within micropores of zeolites: effects of the structure of the active sites and the addition of Pt, J. Phys. Chem. B 101 (1997) 2632-2636.

[73] B. Tahir, M. Tahir, N.S. Amin, Performance analysis of monolith photoreactor for CO_2 reduction with H_2, Energy Convers. Manage. 90 (2015) 272-281.

[74] M.O. Reese, S.A. Gevorgyan, M. Jørgensen, E. Bundgaard, S.R. Kurtz, D.S. Ginley, D.C. Olson, M.T. Lloyd, P. Morvillo, E.A. Katz, A. Elschner, O. Haillant, T.R. Currier, V. Shrotriya, M. Hermenau, M. Riede, K. R. Kirov, G. Trimmel, T. Rath, O. Inganäs, F. Zhang, M. Andersson, K. Tvingstedt, M. Lira-Cantu, D. Laird, C. McGuiness, S. Gowrisanker, M. Pannone, M. Xiao, J. Hauch, R. Steim, D.M. DeLongchamp, R. Rösch, H. Hoppe, N. Espinosa, A. Urbina, G. Yaman-Uzunoglu, J.-B. Bonekamp, A.J.J.M. van Breemen, C. Girotto, E. Voroshazi, F.C. Krebs, Consensus stability testing protocols for organic photovoltaic materials and devices, Sol. Energy Mater. Sol. Cells 95 (2011) 1253-1267.

[75] J.L. Sommerdijk, A. Bril, A.W. de Jager, Two photon luminescence with ultraviolet excitation of trivalent praseodymium, J. Lumin. 8 (1974) 341-343.

[76] P. Harriott, Chemical reactor design, Marcel Dekker Inc, New York, NY, 2003.

[77] G. Wang, B. Wang, J. Park, J. Yang, X. Shen, J. Yao, Synthesis of enhanced hydrophilic and hydrophobic graphene oxide nanosheets by a solvothermal method, Carbon 47 (2009) 68-72.

[78] J. Wu, H. Li, X. Qi, Q. He, B. Xu, H. Zhang, Graphene oxide architectures prepared by molecular combing on hydrophilic-hydrophobic micropatterns, Small 10 (2014) 2239-2244.

[79] L. Sirghi, Y. Hatanaka, Hydrophilicity of amorphous TiO_2 ultra-thin films, Surface Science 530 (2003) L323-L327.

[80] S.S. Tan, L. Zou, E. Hu, Photocatalytic reduction of carbon dioxide into gaseous hydrocarbon using TiO_2 pellets, Catal. Today 115 (2006) 269-273.

Highlights

- CO_2 photoreduction was conducted over graphene oxide/ oxygen-rich TiO_2 under visible light.
- Process parameters such as light intensity as well as CO_2 and H_2O partial pressures were studied.
- A methane yield of 3.45 μmol g_{cat}^{-1} was obtained at the most suitable process conditions.
- Kinetic studies of CO_2 photoreduction over graphene oxide/ oxygen-rich TiO_2 were presented.
- The experimental data was successfully fitted into a dual-site Langmuir-Hinshelwood model.

Graphical Abstract